Degradation Pathways during the Treatment of Methyl tert-Butyl Ether by the UV/H2O2 Process

ARTICLE *in* ENVIRONMENTAL SCIENCE & TECHNOLOGY · FEBRUARY 2000

Impact Factor: 5.33 · DOI: 10.1021/es9905748

3 AUTHORS, INCLUDING:

John Mack
Rhodes University
98 PUBLICATIONS **2,371** CITATIONS
SEE PROFILE

James R Bolton
University of Alberta
315 PUBLICATIONS **9,533** CITATIONS
SEE PROFILE

Environ. Sci. Technol. **2000**, *34,* 650−658

Degradation Pathways during the Treatment of Methyl *tert*-Butyl Ether by the UV/H_2O_2 Process

MIHAELA I. STEFAN,*,†,‡
JOHN MACK,† AND JAMES R. BOLTON†,‡,§
Department of Chemistry, The University of Western Ontario, London, Ontario, N6A 5B7 Canada, and
Calgon Carbon Corporation, 130 Royal Crest Court, Markham, Ontario, Canada L3R 0A1

The application of the UV/H_2O_2 process to the degradation of methyl *tert*-butyl ether (MTBE) in dilute aqueous solution resulted in the generation of *tert*-butyl formate (TBF), 2-methoxy-2-methyl propionaldehyde (MMP), formaldehyde, acetone, *tert*-butyl alcohol (TBA), and methyl acetate as primary byproducts. Other intermediates, such as carbonyl compounds (hydroxy-*iso*-butyraldehyde, hydroxyacetone, pyruvaldehyde) and organic acids (hydroxy-*iso*-butyric, formic, pyruvic, acetic, oxalic) were also detected and quantified during the irradiation. A good organic carbon balance is obtained throughout the treatment, indicating that almost all of the intermediates have been detected. The TOC pattern shows that eventually all the organic compounds are mineralized. Various analytical techniques, such as GC/MS, GC, IC, HPLC, and TOC analysis, were employed in order to identify and quantify the organic products. The detailed reaction mechanism proposed in this study for the degradation of MTBE by •OH-driven oxidation processes accounts for all observed intermediates and the high oxygen demand required for their complete mineralization.

Introduction

During the last two decades, methyl *tert*-butyl ether (MTBE) has been widely used as an additive to gasoline (up to 15%) both to increase the octane number and, as a fuel oxygenate, to improve air quality by reducing the level of carbon monoxide in vehicle exhausts. Despite some benefits of using MTBE as a fuel additive (for example, the reduction by 15% of ozone-forming emissions from vehicles in California in 1996, the state with the worst smog problems in the United States), several concerns have been raised about its impact on human health.

U.S. Geological Survey Data from 1993 to 1994 indicated the presence of MTBE in shallow groundwater in several areas in the United States as a result of contamination from leaking underground gasoline storage tanks. In some cases, the level was up to 1 mg L^{-1} (*1*). Since the concern of public health officials over the presence of MTBE in water is relatively recent, no current regulations on MTBE exist. However, in December 1996, the U.S. EPA tentatively classified it as a possible human carcinogen and issued a draft lifetime health advisory limit of 20−35 μg L^{-1} MTBE in drinking water. In April 1998, the California EPA's Office released a report that proposed a public health goal to limit the level of MTBE in drinking water to 14 μg L^{-1} (*2*).

Squillace et al. (*3*) and Davidson and Parsons (*4*) recently reviewed the current and emerging technologies developed for MTBE-contaminated water remediation. These authors identified advanced oxidation as a promising technology for the treatment of MTBE.

While adsorption on granulated activated carbon (GAC) is very effective in removing MTBE in the 1−100 μg L^{-1} concentration range, advanced oxidation technologies (AOTs) have become a very attractive alternative for contaminated-water remediation at higher MTBE levels (*5*−*12*), since they can provide fast and complete mineralization of the target pollutant and its degradation byproducts, by •OH radical-driven reactions.

MTBE is fairly recalcitrant to treatment by conventional technologies but has a high rate constant for reaction with the •OH radical in aqueous solution [1.6×10^9 M^{-1} s^{-1} (*13*)], so that, under certain conditions, the use of the UV/H_2O_2 process is appropriate.

A literature survey on studies undertaken on the degradation of MTBE initiated by •OH radicals reveals that no complete reaction mechanism has been reported and that very little is known about the use of AOTs in the treatment of MTBE in dilute aqueous solution. Most studies have been conducted in the gas phase, in the presence of methyl nitrite as a light absorber, initiating the process of •OH radical generation (*14*−*19*). Tuazon et al. (*16*) and Smith et al. (*17*) found *tert*-butyl formate (TBF), *tert*-butyl alcohol (TBA), methyl acetate, acetone, and formaldehyde as primary intermediates in the degradation of MTBE, determined their yields of formation, and proposed a detailed mechanism of reaction in the gas phase. Similarly, Japar et al. (*15*) detected TBF, acetone, and formaldehyde as degradation byproducts and, based on a mechanistic approach, suggested that approximately 40% of MTBE should be directly converted to 2-methoxy-2-methyl propionaldehyde (MMP). The latter compound was not, however, detected. Idriss and co-workers (*18*, *19*) conducted the experiments under simulated heterogeneous tropospheric conditions, where TiO_2 and iron oxides were used as photoactive compounds. *iso*-Butene, acetone, formaldehyde, and methanol were reported as degradation intermediates of MTBE.

The use of H_2O_2 for the treatment of MTBE in soil and in solution by Fenton's reaction (dark oxidation) led to TBA and acetone as degradation products (*20*). When a photo-Fenton process was used by Charton et al. (*21*), a *pseudo*-first-order rate constant of 0.069 min^{-1} was measured for the decay of MTBE, and several products were detected, such as TBF, TBA, methyl acetate, acetone, peroxidic material, formaldehyde, alkanes (methane, ethane, *iso*-butane), *iso*-butene, and organic acids (formic, acetic).

Barreto et al. (*22*) have investigated the degradation of MTBE in a TiO_2 heterogeneous aqueous system. On the basis of a product study, a reaction mechanism was proposed that accounts for the detected intermediates, namely, TBF, TBA, acetone, *iso*-butene, *tert*-butyl hydroperoxide, α-hydroperoxy methyl *tert*-butyl ether, acetic acid, and formic acid. A 4-h reaction time was required to remove 1 mM MTBE, and after 10 h, approximately 85% of the initial organic carbon was mineralized.

Kang and Hoffmann (*23*) explored the kinetics and mechanism of the sonolytic destruction of MTBE in the

* Corresponding author telephone: (519)663-3112; fax: (519)663-3067; e-mail: mstefan@boltonuv.com.
† The University of Western Ontario.
‡ Present address: Bolton Photosciences Inc., Siebens Drake Research Institute, 1400 Western Rd., London, ON, N6G 2V4 Canada.
§ Calgon Carbon Corporation.

10.1021/es9905748 CCC: $19.00
Published on Web 12/15/1999

presence of ozone. They found TBF as the only primary oxidation product, which further degrades to acetone and TBA. A first-order rate constant of 4.1×10^{-4} s^{-1} was reported for the decay of 1.0 mM MTBE in aqueous solution.

The only study reported in the literature so far on the removal of MTBE from water by using UV ($\lambda = 254$ nm)/H_2O_2 homogeneous oxidation is that of Wagler et al. (*24*). A maximum rate constant of 0.14 min^{-1} was calculated for the removal of MTBE at pH 6.5, and methanol along with trace amounts of formaldehyde and 1,1-dimethylethyl formate were reported as byproducts.

Considering the environmental concern regarding MTBE and the limited and rather inconsistent literature data with regard to the reaction intermediates generated during the removal of this pollutant, a thorough product study on the degradation of MTBE in dilute aqueous solution using the UV/H_2O_2 process was undertaken. On the basis of the observed and quantified intermediates, we propose a detailed reaction mechanism accounting for the dynamics of the studied system until complete mineralization of all organic compounds initially present or generated during the treatment is achieved. Our next paper (*25*) examines the efficiency of the UV/H_2O_2 process for the treatment of MTBE in contaminated waters.

Experimental Section

Reagents and Materials. All chemicals were analytical reagent grade and used as received from either Sigma-Aldrich or Caledon. Catalase (from bovine liver) was obtained from Sigma and used to destroy the residual H_2O_2 in the collected samples prior to analytical determinations, as described elsewhere (*26*).

Apparatus. The UV irradiation experiments were carried out in a stainless steel 1 kW bench-scale Rayox reactor (manufactured by Calgon Carbon Corporation of Markham, Ontario, Canada), which was described in detail elsewhere (*27*).

The photon flow entering the reactor from the UV−Vis lamp was $(3.82 \pm 0.15) \times 10^{-4}$ einstein s^{-1} in the wavelength range of 200−400 nm, as determined by potassium persulfate actinometry (*28*). The fraction of UV light absorbed within the 200−400-nm range by MTBE, H_2O_2, and $K_2S_2O_8$, individually, was calculated by using a previously developed computer model (*27*).

The reaction volume was 28 L in all experiments and was recirculated at a low flow rate (30 L min^{-1}) in order to avoid any stripping of MTBE and its degradation products. The dissolved oxygen level was monitored during the irradiation with an ATI Orion model 840 DO meter.

Analytical Methods. *Gas Chromatography*. MTBE, TBF, TBA, acetone, methyl acetate, and hydroxyacetone were analyzed by a HP 6890 gas chromatograph system equipped with autosampler. A HP Wax (cross-linked poly(ethylene glycol)) column (30 m × 0.53 mm, 1 μm film thickness) in connection with a flame ionization detector (250 °C) was used. The temperature was programmed at 35 °C for 4 min, then to 150 °C at a rate of 10 °C/min, and held at 150 °C for 2 min; helium was the carrier gas at a flow rate of 16.1 mL min^{-1}. The injector port temperature was 260 °C, and the samples were injected in the split injection mode (split ratio of 10:1).

The oximes, as obtained from the PFBHA derivatization of carbonyl groups according to the procedure described by Le Lacheur et al. (*29*), were analyzed using the same GC system but with a HP-5 (cross-linked 5% PH ME siloxane) column (30 m × 0.32 mm, 0.25 μm film thickness) and an electron capture detector (300 °C). The column temperature was programmed at 50 °C for 1 min, then ramped up to 260 °C at a rate of 5 °C/min, and held there for 2 min; nitrogen was the carrier gas at a flow rate of 3.0 mL min^{-1}. The inlet temperature was 260 °C, and a split injection mode was used at a 10:1 ratio. 2-Methoxy-2-methyl propionaldehyde (MMP) was quantified by using trimethylacetaldehyde (TMA) as a reference compound since no authentic sample of MMP was commercially available.

Ion Chromatography. Organic acids were analyzed by conductivity detection with a Dionex DX-100 ion chromatograph equipped with an anion self-regenerating suppressor ASRS-I and the AI-450 software program. Three different sets of IC conditions were developed in order to fully analyze the complex mixture of acids. An IonPac AS 14 (Dionex, 4 × 250 mm) ion exchange column preceded by an AG 14 guard column (Dionex) was used for the analysis of glycolic, acetic, formic, hydroxy-*iso*-butyric, and pyruvic acids with a 1.8 mM $Na_2B_4O_7$ solution as the eluent (isocratic flow of 1.45 mL min^{-1}). The same column was employed for the analysis of oxalic acid but with 12 mM $Na_2B_4O_7$ as the eluent (isocratic flow of 1.65 mL min^{-1}). Since under the above conditions glyoxylic acid coelutes with acetic acid, the concentration of glyoxylic acid was determined with an IonPac AS 10 (Dionex, 4 × 250 mm) analytical column preceded by a AG 10 guard column (Dionex) with 60 mM NaOH solution as the eluent.

UV−Vis Spectrophotometry. A Hewlett-Packard 8450A diode array spectrophotometer and a 1.00 cm path length quartz cell were used in all absorbance measurements.

Hydrogen peroxide was analyzed spectrophotometrically by the triiodide method (*30*). No other peroxidic material, such as *tert*-butyl hydroperoxide or di-*tert*-butyl peroxide, was found when the same method was applied after H_2O_2 was destroyed by adding catalase.

Gas Chromatography/Mass Spectrometry. Sample Derivatization. The PFBHA [*O*-(2,3,4,5,6-pentafluorobenzyl)hydroxylamine hydrochloride] derivatives of the aldehydes and ketones were obtained as mentioned above. The oxo-acids (hydroxy and/or carbonyl organic acids) were derivatized by a two-step method (*29*) modified as follows: 10 mL reactor sample (pH adjusted to 7) was derivatized by adding 1.6 mL of PFBHA solution (9 mg mL^{-1}), and the reaction was allowed to proceed for 24 h (step 1). H_2SO_4 (96%) was added to ensure a pH < 1.5 so that all carboxylic acids were in their unionized form, followed by a 2-min extraction period in 2.5 mL of MTBE. A total of 200 μL of neat BTSFA [bis-(trimethylsilyl)trifluoroacetamide containing 10% trimethylchlorosilane, TMCS] was added to 1 mL of MTBE extract in screw-cap HP GC vials (suitable for highly volatile compounds), and the derivatization reaction (silylation) was allowed to proceed at 60 °C for 1 h (step 2). Under these conditions, all carbonyl, hydroxyl, and carboxyl functional groups were derivatized as either oximes or trimethylsilyl ethers/esters.

GC/MS Analysis. A Varian 3400 gas chromatograph and a Finnigan MAT mass spectrometer model 8230 were used. A DB-5 fused silica (30 m × 0.25 mm, 0.25 μm film thickness) column was employed, and the temperature was programmed at 50 °C for 1 min, then ramped up to 260 °C at a rate of 10 °C/ min, and held at 260 °C for 3 min. The injector temperature was set to 250 °C, and a split injection mode (10:1 ratio) was chosen. A mass range of 28−600 amu was scanned in all electron ionization mass spectroscopy studies where the electron energy was 70 eV.

The GC/MS method was applied only qualitatively to confirm the identity of the carbonyl and carboxyl compounds generated as intermediates during the UV/H_2O_2 treatment of MTBE. Since very little information is accessible from the GC/MS library database on these types of derivatives, the fragment ions were assigned on the basis of the reference substance mass spectrum where accessible. The studies performed by Glaze et al. (*31*), Le Lacheur et al. (*29*), and Yu et al. (*32*) were a great help.

MMP is one of the expected primary intermediates of the MTBE degradation. Trimethylacetaldehyde (TMA) was used as a surrogate to help in the interpretation of the mass spectrum of the GC peak assigned to MMP. The only difference between the two compounds is the methoxy group in MMP, which replaces a methyl group in TMA. The similar steric configurations and close molecular weights of the PFBHA derivatives of MMP and TMA should translate to similar retention times and fragmentation patterns in the GC/MS analysis. Thus, under the GC/MS conditions mentioned above, retention times of 9.12 and 10.7 min were observed for PFBHA derivatives of TMA (MW = 281 amu) and MMP (MW = 297 amu), respectively. The later observed peak was assigned to MMP on the basis of the mass spectrum analysis, which showed the following specific m/z fragment ions [relative intensities with respect to m/z 181 (100%) are given in brackets, as well]: 282 [$(M - CH_3)^+$, 3.9], 267 [$(M - NO)^+$, 9.7], 266 [$(M - CH_3O)^+$, 5.8], 240 [$(M - C(CH_3)_3)^+$, 19.2], 100 [$(M - OCH_2C_6F_5)^+$, 3.8], 86 [$(M - NOCH_2C_6F_5)^+$, 9.6], 73 [$(CH_3OC(CH_3)_2)^+$, 17.4], 59 [$(HOC(CH_3)_2)^+$, 28.5], 31 [$(CH_3O)^+$, 3.8]. Other fragment ions that are usually encountered in the mass spectra of PFBHA derivatives of aldehydes, such as m/z 182, 161, and 117 (*31*), were present as well.

TOC Analysis. A Shimadzu TOC-5050 analyzer was employed for organic carbon determinations using potassium hydrogen phthalate solutions as TOC standards.

Results and Discussion

A typical experiment for the degradation of MTBE and its intermediates in dilute aqueous solution by the UV/H_2O_2 process is discussed below. The starting concentrations of MTBE and H_2O_2 were 0.92 and 18.26 mM, respectively. Since MTBE does not absorb UV light of $\lambda > 200$ nm and H_2O_2 absorbs 52.2% of the UV light entering the reactor, no direct photolysis of MTBE should be expected. Moreover, dark experiments conducted on a similar MTBE/H_2O_2 mixture did not reveal any thermal reaction occurring between the two compounds. Consequently, all degradation processes must be induced by the direct photolysis of hydrogen peroxide, which provides highly oxidizing •OH radicals.

MTBE Decay and Degradation Intermediates. Figure 1a shows the MTBE decay and some of the primary intermediates observed during the treatment under the conditions stated above.

Since MTBE is oxidized by the •OH radical with a high rate constant (1.6×10^9 M^{-1} s^{-1}), it decays very rapidly following *pseudo*-first-order kinetics with an observed rate constant of $k = (5.79 \pm 0.32) \times 10^{-3}$ s^{-1}. Several major primary reaction products, such as TBF, TBA, acetone, methyl acetate, 2-methoxy-2-methyl propionaldehyde, and formaldehyde, are generated and further oxidized to aldehydes and/or the corresponding acids, whose time profiles are shown in Figure 1, panels b and c. Note that acetone reaches the highest concentration as compared to other early intermediates. That suggests not only that acetone is a less reactive organic compound toward •OH radicals, but also that it is generated from some of the MTBE byproducts. Formaldehyde reacts very rapidly with hydroxyl radicals, but its time profile suggests that it is also a degradation byproduct of the early-generated intermediates.

Pyruvaldehyde, hydroxyacetone, hydroxy-*iso*-butyraldehyde, and formic, hydroxy-*iso*-butyric, pyruvic, acetic, and oxalic acids were identified and measured as degradation byproducts of the primary intermediates. Low concentrations of acetaldehyde, *iso*-butyraldehyde, glycolic, and glyoxylic acids (less than 0.02 mM) were also measured among the byproducts.

A few products, such as 2,5-dimethoxy-2,5-dimethyl hexane and *tert*-butoxy-*iso*-propoxy methane (coupling products), hydroxymethyl *tert*-butyl ether, 1,1-dimethylethyl acetate, and 3-methoxy-3-methyl 2-butanone, were detected by GC/MS analysis during the early stages of the irradiation but were not quantified since no authentic samples were commercially available. However, they appear to be at extremely low levels as compared with the measured byproducts. All these intermediates can be mechanistically predicted.

The decay of hydrogen peroxide exhibited zero-order kinetics at a rate of $(5.16 \pm 0.12) \times 10^{-6}$ M s^{-1}, which is lower than that determined for the photolysis of H_2O_2 alone [$(6.60 \pm 0.02) \times 10^{-6}$ M s^{-1}]. This arises from the fact that MTBE and its degradation intermediates compete with H_2O_2 for the •OH radicals. The pattern of H_2O_2 decay is shown in Figure 2.

The degradation of MTBE and the generation of primary intermediates are highly oxygen demanding processes, as indicated by the pattern of the O_2 concentration (Figure 2). The O_2 level increases by the end of the irradiation period as a result of the efficient competition of H_2O_2 for the •OH radicals.

Total Organic Carbon Balance (TOC). Figure 2 depicts the pattern of TOC experimentally measured versus that calculated by adding up the organic carbon contained by the intermediates identified and quantified by various analytical methods.

We consider that, given such a complicated system, there is a good agreement between the two TOC curves; this indicates that most of the byproducts were identified and properly quantified. The discrepancy of about maximum 10% observed between the calculated and measured TOC in the region of 2−20 min irradiation times could be accounted for by a few aldehydes and coupling products detected but not quantified, which may be high carbon level containing intermediates. As mentioned above, their concentrations must be extremely low.

The TOC data confirm that all of the organic compounds are mineralized when the UV/H_2O_2 process is applied to the MTBE removal.

Degradation of Reaction Intermediates. The UV/H_2O_2 process was applied individually to some of the most important byproducts generated during the MTBE treatment, namely TBF, TBA, and acetone, to obtain a complete and reliable picture of the reaction sequence.

TBF Degradation. A 0.92 mM TBF and 10 mM H_2O_2 aqueous solution was irradiated under the same conditions as used for the MTBE treatment. Acetone and formaldehyde were the major primary byproducts. Formic acid, hydroxy-*iso*-butyraldehyde, and very low levels of TBA were detected as primary intermediates as well, whereas pyruvaldehyde, hydroxyacetone, and hydroxy-*iso*-butyric, pyruvic, acetic, and oxalic acids were measured as further byproducts.

The pattern of the O_2 level during the decay of TBF was similar to that observed in the case of MTBE. A good carbon balance was obtained during the entire irradiation period (80 min), and all the organic compounds were eventually mineralized.

TBA Degradation. A 0.55 mM TBA solution in the presence of 10 mM H_2O_2 was irradiated until complete removal of any organic compound was achieved. Acetone, formaldehyde, and hydroxy-*iso*-butyraldehyde were the primary intermediates, whereas pyruvaldehyde, formic, hydroxy-*iso*-butyric, pyruvic, acetic, and oxalic acids were generated in the system as a result of further oxidation processes. Low levels of hydroxyacetone were also quantified. A very good organic carbon balance was obtained during the irradiation period (60 min).

According to the product studies carried out on the degradation of TBF and TBA by the UV/H_2O_2 process, acetone is the major intermediate generated in both cases. The degradation of acetone and intermediates generated using

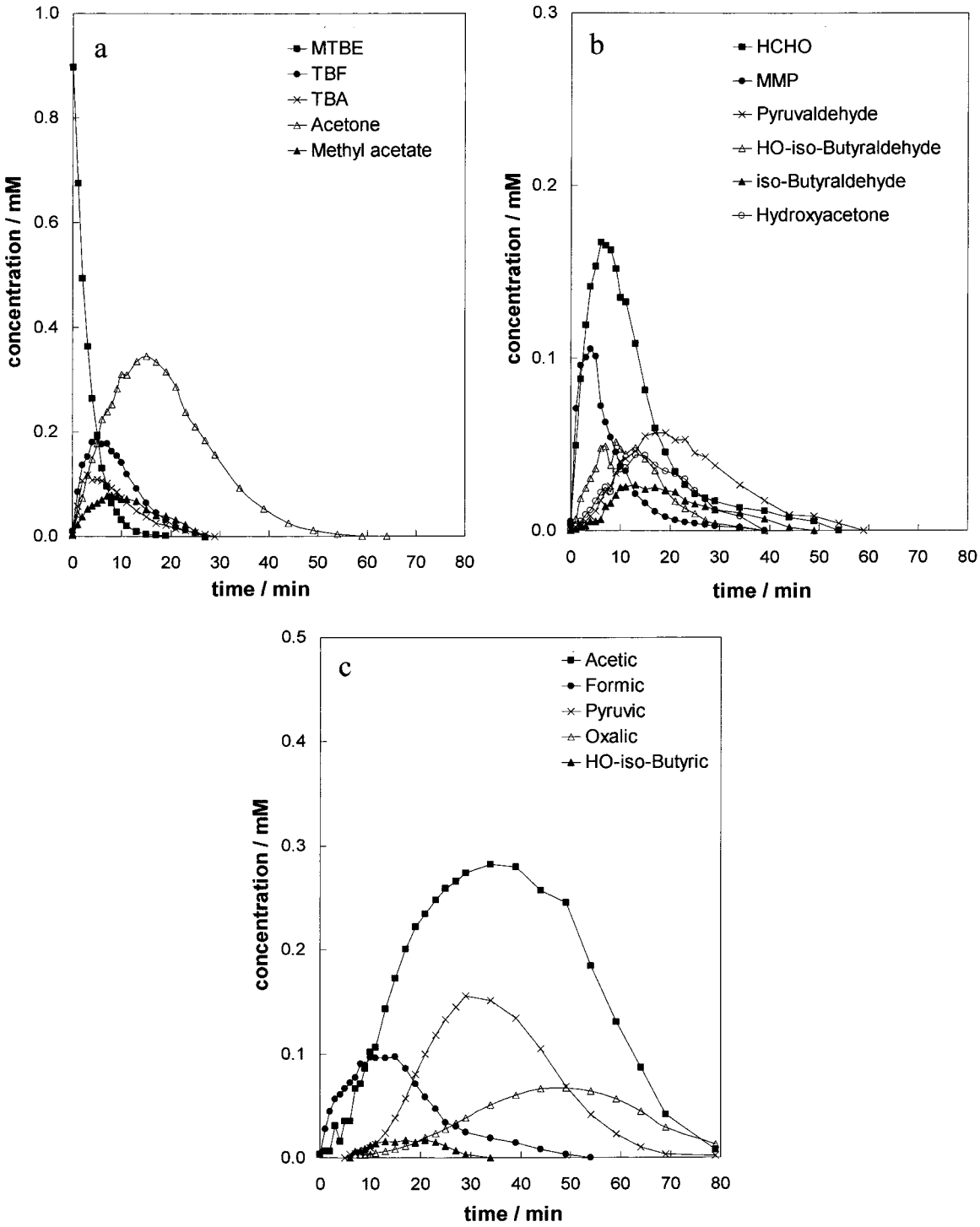

FIGURE 1. Time profiles for the decay of MTBE and its intermediates ($[H_2O_2]_o$ = 18.26 mM). (a) MTBE and some primary intermediates; (b) carbonyl compounds (except acetone); (c) carboxylic acids.

the same oxidation process has been described in detail elsewhere (*26, 27*).

Degradation Pathways during the UV/H_2O_2 Treatment of MTBE. The following proposed mechanism accounts for the experimentally observed major intermediates. In such a complex system, more reactions can be expected, but they may account only for the generation of the minor byproducts. They will not be described in the discussion below.

Generation of Primary Intermediates. Scheme 1 shows the primary processes occurring in the treatment of MTBE. Direct photolysis of H_2O_2 is the only photochemical step in the entire reaction mechanism and results in the generation of hydroxyl radicals with a quantum yield of 1.0.

Hydroxyl radical attack by H-abstraction can take place at either the methoxy group or any of the three equivalent methyl groups in the MTBE molecule leading to carbon-centered radicals:

$$(CH_3)_3C\text{-}OCH_3 + {}^{\bullet}OH \rightarrow (CH_3)_3C{-}OCH_2^{\bullet} + H_2O \quad (1)$$

$$CH_3OC(CH_3)_2CH_3 + {}^{\bullet}OH \rightarrow CH_3OC(CH_3)_2CH_2^{\bullet} + H_2O \quad (2)$$

It is well-known that the $^{\bullet}OH$ radical is an electrophile and that C−H bonds adjacent to oxygen are responsible for a pronounced stereoelectronic effect that produces high rates

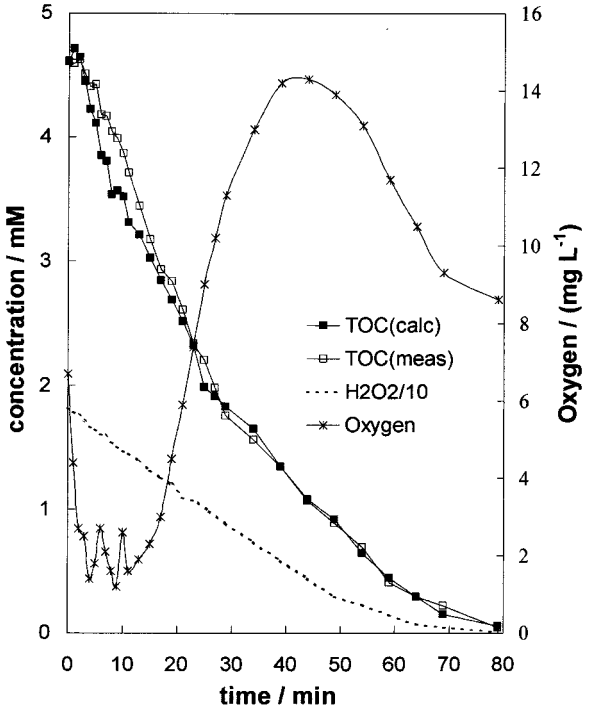

FIGURE 2. Total organic carbon (TOC) balance and H_2O_2 decay.

SCHEME 1. Primary Processes in the MTBE Degradation

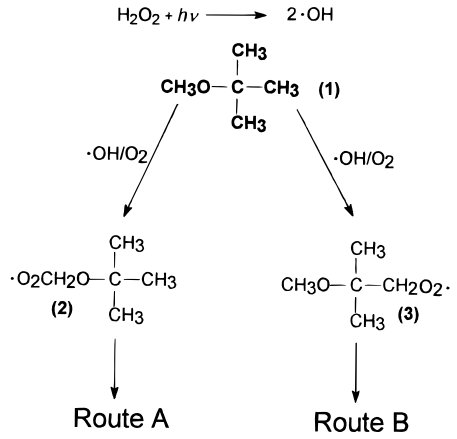

of H-atom abstraction. Therefore, the H atoms in the methoxy group of MTBE molecule are most prone to radical attack (reaction 1 and route A).

The carbon-centered radicals generated in reactions 1 and 2 will react with oxygen at diffusion-controlled rate constants ($\sim 10^9-10^{10}$ M^{-1} s^{-1}) generating peroxyl radicals (**2**) and (**3**), respectively (Scheme 1). The chemistry of peroxyl radicals in aqueous solution has been extensively studied in the literature during the last two decades (*33*−*37*).

At high concentrations of the parent molecule, peroxyl radicals can initiate autoxidative chain reactions by H-abstraction leading to hydroperoxides. Under the conditions used in this study, such reactions cannot proceed. Since no detectable peroxidic organic material was found, we assume that the peroxyl radicals generated in the investigated system undergo primarily head-to-head termination reactions.

Schemes 2 and 3 show the proposed mechanism for the generation of the primary detected intermediates, which involves two different pathways (routes A and B, respectively), corresponding to the two possible sites for the attack of the •OH radicals on the MTBE molecule. The tetroxides (**4**) and (**12**) in routes A and B, respectively, were formed by self-

SCHEME 2. Degradation Pathways through Route A

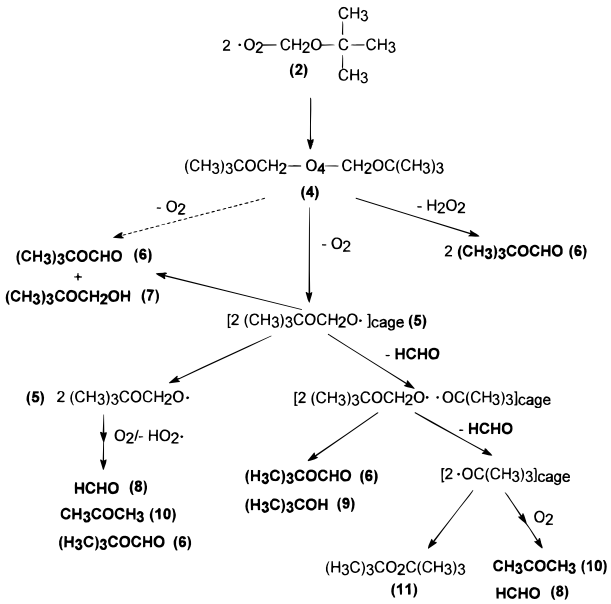

SCHEME 3. Degradation Pathways through Route B

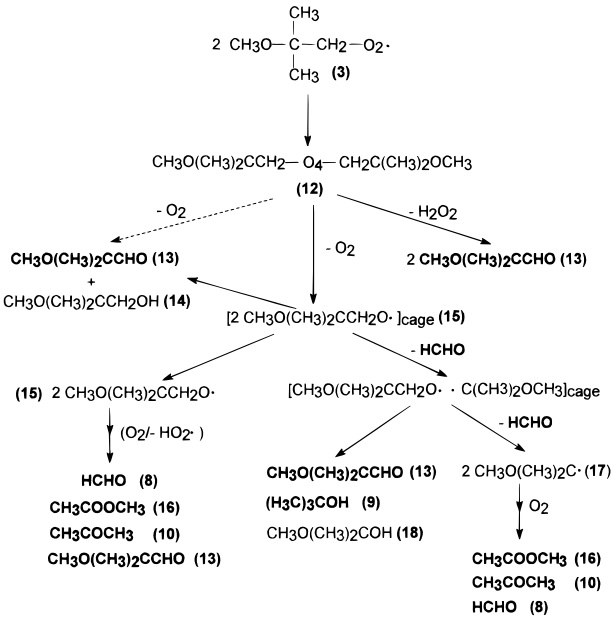

termination reactions of the corresponding peroxyl radicals. Cross-termination reactions between peroxyl radicals (**2**) and (**3**) are also highly possible, and a 'mixed' tetroxide $(CH_3)_3$-$COCH_2$-O_4-$CH_2C(CH_3)_2OCH_3$ will be involved. This decays through patterns similar to routes A and B, when the same major intermediates will be generated.

It is generally accepted that a tetroxide intermediate can decay by two distinct pathways: concerted processes and free-radical processes [see von Sonntag and Schuchmann (*34*, *38*) and references therein].

In route A, the reaction intermediates as expected from concerted processes should be *tert*-butyl formate (TBF) (**6**) and hydroxymethyl *tert*-butyl ether (**7**). Since a very small peak of (**7**) was seen in GC/MS analysis, but TBF was measured as a major primary product, we assume that Russell mechanism (*39*) does not play an important role in this system. On the other hand, hydroxymethyl *tert*-butyl ether (**7**) should react very fast with •OH radicals by H-abstraction at the substituted methoxy, highly activated by both ether and hydroxyl groups.

The generation of 2-methoxy-2-methyl propionaldehyde (MMP) (**13**) is a source of controversy in the published literature, as mentioned in the Introduction. However, our study indicated the presence of low levels of this aldehyde as a primary degradation byproduct generated through route B. Along with methyl acetate, the detection of MMP proves the occurrence of •OH radical attack on the methyl group of the *tert*-carbon in MTBE.

Similar to route A, the decay of the tetroxide (**12**) in route B by the Russell mechanism should not be important, since the alcohol (**14**) was not identified. *neo*-Pentyl alcohol was used as a surrogate for (**14**) in GC and GC/MS analyses, given their similar structures.

Formaldehyde (**8**), acetone (**10**), and TBA (**9**) in routes A and B, and in addition, methyl acetate (**16**) in route B, are also primary intermediates (Figure 1, panels a and b), since they are generated directly from MTBE at short irradiation times. These compounds are formed from alkoxyl radicals **5** and **15**, respectively, which indicates that the decay of the corresponding tetroxides through free-radical processes is significant.

Since some of the primary intermediates are common to both routes, it is difficult to ascertain a branching ratio among the various paths. However, a rough estimate can be made at very short irradiation times, when the primary intermediates are not expected to compete with MTBE for •OH radicals. For example, within the first minute of irradiation, the MTBE decayed by 0.22 mM, whereas approximately 0.085 mM TBF, 0.05 mM MMP, and 0.02 mM methyl acetate were quantified among the primary intermediates. Assuming that methyl acetate and acetone are generated in equimolar amounts from the alkoxyl radical (**15**) (see the detailed mechanism below), at least 40% of MTBE decays as a result of •OH attack at the *tert*-butyl side, and thus ~60% of it isdue to •OH attack at the methoxy group. That implies a ~3:2 branching ratio between the two possibilities of •OH attack on MTBE, which is in a good agreement with the ratio estimated from the rate constants in the gas phase (*40*). The ~40% generation of TBF implies that about two-thirds of the MTBE decaying by the •OH radical attack at the methoxy group leads to TBF.

The pathways leading to alkoxyl radicals in routes A and B are important, as judged from the level of HCHO at early irradiation times. Again, a rough estimate leads to the conclusion that ~40% of MTBE should decompose through alkoxyl radical pathways.

The alkoxyl radicals (**5**) in route A and (**15**) in route B can disproportionate in the solvent cage, leading to the same products as those generated by the decay of the tetroxides (**4**) and (**12**) through Russell mechanism, respectively. As mentioned before, the disproportionation reactions of radicals (**5**) and (**15**) to form the alcohols (**7**) and (**14**) appear not to play an important role.

Instead, the elimination of a formaldehyde molecule from one alkoxyl radical by β-scission (reaction 3) followed by disproportionation in solvent cage (reaction 4) seem to be the mechanisms for the generation of TBA in routes A and B and of 2-methoxy-2-methyl propanol (**18**) (not detected) in route B. The time profiles of TBF and TBA during irradiation support the proposed mechanism:

$$[2(CH_3)_3C\text{-}O\text{-}CH_2O^\bullet]_{cage} \rightarrow HCHO + [(CH_3)_3C\text{-}O\text{-}CH_2O^\bullet\ {}^\bullet OC(CH_3)_3]_{cage} \quad (3)$$

$$[(CH_3)_3C\text{-}O\text{-}CH_2O^\bullet\ {}^\bullet OC(CH_3)_3]_{cage} \rightarrow (CH_3)_3C\text{-}O\text{-}CHO + (CH_3)_3C\text{-}OH \quad (4)$$

The loss of the second molecule of HCHO followed by either cage recombination or escape from the cage would result in formation of di-*tert*-butyl peroxide (**11**, not detected) or *tert*-butoxyl radicals. Similar cage recombination reactions are expected in the generation of the byproducts outlined in route B.

Escaped from the solvent cage, the alkoxyl radicals (**5**, route A; **15**, route B) can undergo either β-scission or 1,2-H shift to carbon-centered radicals. β-Scission in radical (**5**) leads to formaldehyde (**8**) and the *tert*-butoxyl radical (reaction 5), which in turn follows either first-order (reaction 6) or *pseudo*-first-order decay (reaction 7):

$$(CH_3)_3C\text{-}O\text{-}CH_2O^\bullet \rightarrow HCHO + (CH_3)_3CO^\bullet \quad (5)$$

$$(CH_3)_3CO^\bullet \rightarrow (CH_3)_2CO + CH_3^\bullet \quad (6)$$

$$(CH_3)_3CO^\bullet + R\text{-}H \rightarrow (CH_3)_3COH + R^\bullet \quad (7)$$

The *tert*-butoxyl radical loses a methyl radical [$\tau \sim 1\ \mu$s (*41*)] leading to acetone (**10**) (Scheme 2 and reaction 6) as a primary product. Methyl radicals react rapidly with O_2 to generate primarily formaldehyde (*42*). The extent of reaction 7 is expected to be very low as compared to fragmentation 6, because of the rather small rate constant (10^4–$10^5\ M^{-1}\ s^{-1}$) and the low concentration of RH (MTBE, acetone, $HO_2^\bullet$ radicals) present in the system. This is consistent with the high level of acetone concentration as compared to that of TBA observed in the present study.

Similarly, the alkoxyl radical (**15**) in route B loses formaldehyde by β-scission, and the carbon-centered radical (**17**) is generated (reaction 8). This reacts with O_2 leading to a tertiary peroxyl radical (reaction 9), which decomposes to a *tert*-alkoxyl radical (reaction 10). A 1,2-methyl shift in the carbon-centered radical (**17**) with the formation of *tert*-butoxyl radical is highly possible (reaction 11). This may explain the absence of 2-methoxy-2-methyl propanol (**18**) in the investigated system:

$$CH_3O(CH_3)_2C{-}CH_2O^\bullet \rightarrow HCHO + CH_3O(CH_3)_2C^\bullet \quad (8)$$

$$CH_3O(CH_3)_2C^\bullet + O_2 \rightarrow CH_3O(CH_3)_2CO_2^\bullet \quad (9)$$

$$2CH_3O(CH_3)_2CO_2^\bullet \rightarrow 2CH_3O(CH_3)_2CO^\bullet + O_2 \quad (10)$$

$$CH_3O(CH_3)_2C^\bullet \rightarrow (CH_3)_3CO^\bullet \quad (11)$$

In general, the bimolecular decay of tertiary peroxyl radicals is much slower than that of primary and secondary ones. The corresponding tetroxide will not decay through Russell (*39*) or Bennett (*43*) mechanisms. Depending on the fragmentation route, the alkoxyl radical generated in reaction 10 leads primarily to either acetone (**10**) or methyl acetate (**16**).

A very well-known reaction of primary and secondary alkoxyl radicals is isomerization by a 1,2-H shift to a carbon-centered radical. These reactions have half-lives of less than 1 μs and are water-assisted processes. Von Sonntag and Schuchmann (*33*) indicate that the 1,2-H shift is so fast that it usually prevails over fragmentation reactions. Therefore, the alkoxyl radical (**5**) in route A should undergo the isomerization reaction 12, followed by reaction of the carbon-centered radical with O_2 (reaction 13):

$$(CH_3)_3C\text{-}O\text{-}CH_2O^\bullet \rightarrow (CH_3)_3C\text{-}O\text{-}CH(OH)^\bullet \quad (12)$$

$$(CH_3)_3C\text{-}O\text{-}CH(OH)^\bullet + O_2 \rightarrow (CH_3)_3C\text{-}O\text{-}CH(OH)O_2^\bullet \quad (13)$$

$$(CH_3)_3C\text{-}O\text{-}CH(OH)O_2^\bullet \rightarrow (CH_3)_3C\text{-}O\text{-}CHO + HO_2^\bullet \quad (14)$$

The α-hydroxy alkoxyalkyl peroxyl radical generated in reaction 13, activated by the ether function, eliminates $HO_2^\bullet$

spontaneously via a five-membered cyclic transition state, leading to TBF (**6**) (reaction 14 and Scheme 2).

Following similar reactions, the alkoxyl radical (**15**) in route B generates 2-methoxy-2-methyl propionaldehyde (**13**). However, as a highly branched radical, the alkoxyl radical (**15**) is expected to undergo primarily β-scission reaction 8.

Thus, both TBF and MMP can be generated through various pathways starting from the peroxyl radicals (**2**) and (**3**), respectively. However, it is impossible to distinguish between the concerted and the free-radical mechanisms, which lead to the same products.

At the irradiation times where most of the MTBE was removed from the solution, the peroxyl radicals generated from its byproducts become good 'candidates' for cross-termination reactions of peroxyl radicals (**2** and **3**). For instance, the reactions with the acetonyl peroxyl radical CH_3-$COCH_2O_2^{\bullet}$ lead to some of the observed reaction products, such as TBF, MMP, hydroxyacetone, pyruvaldehyde, formaldehyde, acetic acid (measured), acetaldehyde, 1,1-dimethylethyl acetate, and 3-methoxy-3-methyl 2-butanone (identified at very low levels, but not quantified). The following reactions could generate some of the acetic acid present in the system at short irradiation times:

$$[(CH_3)_3C\text{-}O\text{-}CH_2O^{\bullet}\ {}^{\bullet}OCH_2COCH_3]_{cage} \xrightarrow{-2HCHO} (CH_3)_3C\text{-}O\text{-}C(O)CH_3 \xrightarrow{H_2O} CH_3COOH + (CH_3)_3C\text{-}OH \quad (15)$$

$$[(CH_3)_3C\text{-}O\text{-}CH_2O^{\bullet}\ {}^{\bullet}OCH_2COCH_3]_{cage} \xrightarrow{-HCHO} (CH_3)_3C\text{-}O\text{-}CHO + CH_3CHO \quad (16)$$

The degradation mechanisms of the major primary intermediates observed in the treatment of MTBE are briefly given below. Even though similar concepts regarding the formation and decay of tetroxides apply, mostly the free-radical processes will be discussed.

Degradation of TBF. The papers published in the literature on the degradation of MTBE explain the decay of *tert*-butyl formate by an acid-catalyzed hydrolysis to TBA. Studies carried out on the thermal stability of a 1 mM TBF solution at pH 4.0 and pH 6.8 indicated no change in the concentrations of TBF or TBA (initially present as ~5% in TBF samples), neither in the presence nor in the absence of H_2O_2 over 24 h, whereas 4% of the initial concentration of TBF was hydrolyzed to TBA within 10 min at pH 3.0. Therefore, we believe that no significant hydrolysis of TBF (maximum concentration reached in the system of ~0.2 mM) to TBA and formic acid can occur in the time scale and pH range of our irradiation experiments. Moreover, the degradation of TBF by $^{\bullet}OH$ radical-driven processes [$k = (4.1 \pm 0.2) \times 10^8$ M^{-1} s^{-1} (*44*)] should definitely prevail over hydrolysis.

In mildly acidic conditions (non-hydrolytic), *tert*-butyl esters yield carboxylic acids and *iso*-butene through a stable *tert*-carbocation as an intermediate (water-assisted process). However, as pointed out above, no significant level of thermal reaction of TBF was determined over the pH range measured during the irradiation experiments (3.3−5.0). In conclusion, we believe TBF decays primarily by $^{\bullet}OH$ attack, as shown in Scheme 4.

There are two possible sites for H-atom abstraction by $^{\bullet}OH$ radicals. The attack at formoyl group seems to be more likely than at one of the three equivalent methyl groups on the *tert*-butyl side, given the charge distribution and electrophilic character of $^{\bullet}OH$ radical. The carbon-centered radical (**19**) reacts with O_2 and, through a peroxyl radical intermediate, generates acetone (**10**), formaldehyde (**8**), and CO_2. This is the main route of the TBF degradation.

H-abstraction from the *tert*-butyl side forms the carbon-centered radical (**20**). The reactions of the corresponding

SCHEME 4. TBF Degradation Pathways

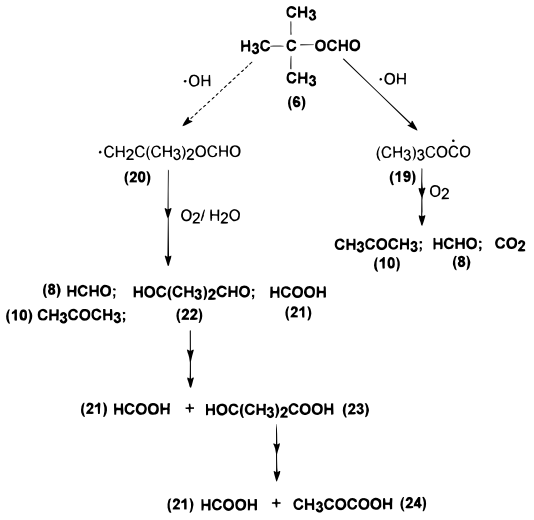

alkoxyl radical, either in the solvent cage or as escaped from the cage, account for the observed degradation products of TBF.

Cross-termination reactions between peroxyl radicals generated from TBF and acetone may lead to TBA and acetic acid at short irradiation times (reactions 17 and 18):

$$[(CH_3)_3C\text{-}O\text{-}C(O)O^{\bullet}\ {}^{\bullet}OCH_2COCH_3]_{cage} \xrightarrow{-CO_2} (CH_3)_3C\text{-}OH + CH_3COCHO \quad (17)$$

$$[(CH_3)_3C\text{-}O\text{-}C(O)O^{\bullet}\ {}^{\bullet}OCH_2COCH_3]_{cage} \xrightarrow{-HCHO/-CO_2} (CH_3)_3C\text{-}O\text{-}C(O)CH_3 \xrightarrow{H_2O} (CH_3)_3C\text{-}OH + CH_3COOH \quad (18)$$

However, the above reactions proceed at a very low extent as compared to those leading to acetone, which is consistent with the patterns of the generated intermediates, where no significant growth of TBA was observed, suggesting that TBA is a minor degradation product of TBF.

Degradation of MMP. Since 2-methoxy-2-methyl propionaldehyde is not commercially available, no product study was conducted in this case. However, based on the observed intermediates, a simplified reaction mechanism for the degradation of MMP involving $^{\bullet}OH$ radicals is proposed in Scheme 5.

As generally accepted, aldehydes exist in solution mainly in their hydrated forms. H-abstraction at the carbonyl site of **25**, followed by further oxidation, would lead to 2-methoxy-2-methyl propionic acid (**26**). The methoxy group in **26** should be the preferred attack site for the $^{\bullet}OH$ radical forming the carbon-centered radical (**27**). The alkoxyl radical generated from **27** can undergo either fragmentation (reactions 19−22) or 1,2-H shift (reaction 23), leading to the corresponding products as outlined by the two routes in Scheme 5:

$$^{\bullet}OCH_2\text{-}OC(CH_3)_2COOH \rightarrow HCHO + {}^{\bullet}OC(CH_3)_2COOH \quad (19)$$

$$^{\bullet}OC(CH_3)_2COOH \rightarrow CH_3COCH_3 + {}^{\bullet}CO_2^- + H^+ \quad (20)$$

$$^{\bullet}CO_2^- + O_2 \xrightarrow{H^+} CO_2 + HO_2^{\bullet}/\ O_2^{\bullet -} \quad (21)$$

$$^{\bullet}OC(CH_3)_2COOH \rightarrow CH_3COCOOH + {}^{\bullet}CH_3 \quad (22)$$

$$^{\bullet}O_2(HO)CH\text{-}OC(CH_3)_2COOH \xrightarrow[H_2O]{-HO_2^{\bullet}} HCOOH + HOC(CH_3)_2COOH \quad (23)$$

SCHEME 5. MMP Degradation Pathway

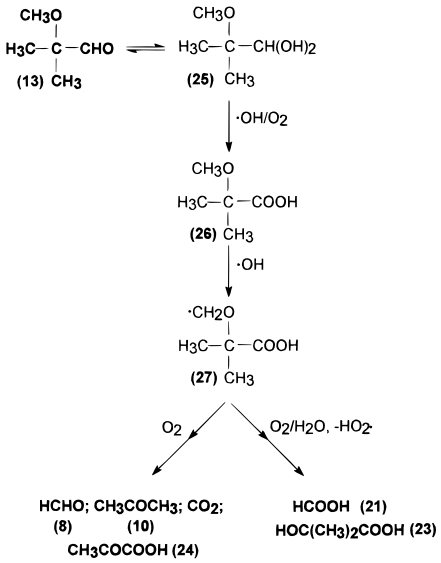

SCHEME 6. TBA Degradation Pathways

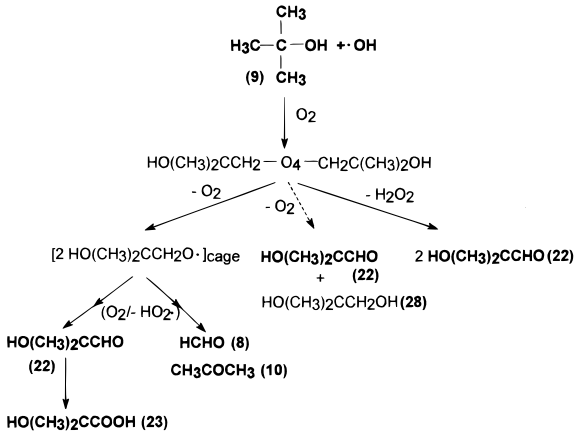

The attack of the •OH radical at the methoxy group (less favored) in **25** will lead to pyruvaldehyde and formaldehyde as major products.

Degradation of TBA. A thorough pulse radiolysis study on the degradation of *tert*-butyl alcohol was reported by Schuchmann and von Sonntag (*38*). Since in pulse radiolysis the concentrations of the reactive species are much higher than those reached in our UV irradiation study, not all products listed in this paper were observed in the present study. Scheme 6 gives the simplified reaction mechanism proposed for the degradation of TBA.

Note that no thermal reaction occurred in a TBA−H_2O_2 aqueous solution within the investigated pH range (3−7). Consequently, *iso*-butene, which was proposed by Barreto et al. (*22*) as being formed from TBA, was not detected. This is consistent with the reaction mechanism for dehydration of *tert*-alcohols, where strong acidic media (40−50% H_2SO_4) and high temperatures (85 °C) are required.

The attack of the •OH radical on TBA [$k = 6 \times 10^8$ M^{-1} s^{-1} (*13*)] occurs primarily (95%) at one of the three equivalent methyl groups (*45*). Formaldehyde, acetone, and hydroxy-*iso*-butyraldehyde are the major primary degradation intermediates. The low levels of hydroxy-*iso*-butyraldehyde and its corresponding carboxylic acid are due to their high reactivity toward the •OH radical. This concept is strongly supported by the observation of a high level of pyruvic acid generated in the degradation of TBA by the UV/H_2O_2 process, where it can be formed not only from acetone (*26*) but also as a direct degradation product of hydroxy-*iso*-butyric acid through the corresponding alkoxyl radical (reactions 24 and 25):

$$^{\bullet}OCH_2\text{-}(HO)C(CH_3)COOH \rightarrow HCHO + {}^{\bullet}(HO)C(CH_3)COOH \quad (24)$$

$$^{\bullet}(HO)C(CH_3)COOH + O_2 \xrightarrow{-HO_2^{\bullet}} CH_3COCOOH \quad (25)$$

Pyruvate ion has a smaller rate constant for reaction with the •OH radical [$k = 3.1 \times 10^7$ $M^{-1}s^{-1}$ (*13*); p$K_a = 2.93$] than the other organic compounds present in the system at early irradiation times, so it cannot compete for •OH radicals and builds up in solution. As shown elsewhere (*26*), pyruvic acid leads to acetic acid, by both a thermal reaction with H_2O_2 and by reaction with •OH radicals. Consequently, there are various sources of acetic acid during the treatment of MTBE by the UV/H_2O_2 process, which may explain the rather high level reached during the irradiation.

Degradation of Acetone. A detailed reaction mechanism for the decay of acetone and its reaction intermediates (by the UV/H_2O_2) treatment until the complete mineralization of each organic compound is achieved is given elsewhere (*26*, *27*).

Acknowledgments

This work was supported financially by a Collaborative Research and Development Grant jointly funded by the Natural Science and Engineering Research Council of Canada and Calgon Carbon Corporation, Markham, Ontario, Canada. We are grateful to Dr. Stephen Cater, Mr. Keith Bircher, P. Eng. and Dr. Ali Safarzadeh-Amiri of Calgon Carbon Corporation for their helpful comments and support during the conduct of this research. We extend our thanks to Dr. Bertrand Dussert of Calgon Carbon Corporation, Pittsburgh, PA, for his kind assistance with this project. Also, we wish to express our appreciation for the technical assistance of Dr. Dave Budac and Mr. Doug Hairsine.

Literature Cited

(1) Leclair, V. *Environ. Sci. Technol.* **1997**, *31*, 176A.
(2) Lovett, R. A. *Environ. Sci. Technol.* **1998**, *32*, 304A.
(3) Squillace, P. J.; Pankow, J. F.; Korte, N. E.; Zogorski, J. S. *Environ. Toxicol. Chem.* **1997**, *16*, 1836.
(4) Davidson, J. M.; Parsons, R. In *Proceedings of the Petroleum Hydrocarbons and Organic Chemicals in Ground Water: Prevention, Detection, and Remediation Conference*, November 13−15, 1996; Ground Water Publishing Company: Houston, TX, 1996; pp 15−29.
(5) Ollis, D. F.; Pelizzetti, E.; Serpone, N. *Environ. Sci. Technol.* **1991**, *25*, 1523.
(6) von Sonntag, C.; Mark, G.; Mertens, R.; Schuchmann, H.-P.; Schuchmann, M. N. *J. Water SRT-Aqua* **1993**, *42*, 201.
(7) Legrini, O.; Oliveros, E.; Braun, A. M. *Chem. Rev.* **1993**, *93*, 671.
(8) Masten, S. J.; Davies, S. H. R. In *Environmental Oxidants*; Nriagu, J. O., Simmons, M. S., Eds.; Wiley: New York, 1994; pp 517−548.
(9) Bolton, J. R.; Cater, S. R. In *Aquatic and Surface Photochemistry*; Helz, G. R., Zepp, R. G., Crosby, D. G., Eds.; Lewis: Boca Raton, FL, 1994; pp 467−490.
(10) Prousek, J. *Chem. Listy* **1996**, *90*, 307.
(11) Rajeshwar, K. *Chem. Ind.* **1996**, 454.
(12) Venkatadri, R.; Peters, R. W. *Hazard. Waste Hazard. Mater.* **1997**, *10*, 107.
(13) Buxton, G. V.; Greenstock, C. L.; Helman, W. P.; Ross, A. P. *J. Phys. Chem. Ref. Data* **1988**, *17*, 513.
(14) Wallington, T. J.; Dagaut, P.; Liu, R.; Kurylo, M. J. *Environ. Sci. Technol.* **1988**, *22*, 842.
(15) Japar, S. M.; Wallington, T. J.; Richert, J. F. O.; Ball, J. C. *Int. J. Chem. Kinet.* **1990**, *22*, 1257.
(16) Tuazon, E. C.; Carter, W. P. L.; Aschmann, S. M.; Atkinson, R. *Int. J. Chem. Kinet.* **1991**, *23*, 1003.
(17) Smith, D. F.; Kleindienst, T. E.; Hudgens, E. E.; McIver, C. D.; Bufalini, J. J. *Int. J. Chem. Kinet.* **1991**, *23*, 907.

(18) Idriss, H.; Seebauer, E. G. *J. Vac. Sci. Technol., A* **1996**, *14*, 1627.
(19) Idriss, H.; Miller, A.; Seebauer, E. G. *Catal. Today* **1997**, *33*, 215.
(20) Yeh, C. K.; Novak, J. T. *Water Environ. Res.* **1995**, *67*, 828.
(21) Charton. N.; Guillard, C.; Hoang-Van, C.; Pichat, P. *PSI−Proc.* **1997**, *97−02*, 65.
(22) Barreto, R. D.; Gray, K. A.; Anders, K. *Water Res.* **1995**, *29*, 1243.
(23) Kang, J.-W.; Hoffman, M. R. *Environ. Sci. Technol.* **1998**, *32*, 3194.
(24) Wagler, J. L.; Malley, J. P., Jr. *J. N. Engl. Water Works Assoc.* **1994**, *108*, 236.
(25) Safarzadeh-Amiri, A.; Cater, S. R.; Stefan, M. I.; Bolton, J. R. *Environ. Sci. Technol.*, **2000**, *34*, 659−662.
(26) Stefan, M. I.; Bolton, J. R. *Environ. Sci. Technol.* **1999**, *33*, 870.
(27) Stefan, M. I.; Hoy, A. R.; Bolton, J. R. *Environ. Sci. Technol.* **1996**, *30*, 2382.
(28) Mark, G.; Schuchmann, M. N.; Schuchmann, H.-P.; von Sonntag, C. *J. Water SRT-Aqua* **1990**, *39*, 309.
(29) Le Lacheur, R. M.; Sonnenberg, L. B.; Singer, P. C.; Christman, R. F.; Charles, M. J. *Environ. Sci. Technol.* **1993**, *27*, 2745.
(30) Klassen, N. V.; Marchington, D.; McGowan, H. C. E. *Anal. Chem.* **1994**, *66*, 2921.
(31) Glaze, W. H.; Koga, M.; Cancilla, D. *Environ. Sci. Technol.* **1989**, *23*, 838.
(32) Yu, H.; Flagan, R. C.; Seinfeld, J. H. *Environ. Sci. Technol.* **1998**, *32*, 2357.
(33) von Sonntag, C.; Schuchmann, H.-P. *Angew. Chem., Int. Ed. Engl.* **1991**, *30*, 1229.
(34) von Sonntag, C.; Schuchmann, H.-P. In *Peroxyl Radicals*; Alfassi, Z. B., Ed.; Wiley: Chichester, U.K., 1997; pp 173−234.
(35) von Sonntag, C.; Dowideit, P.; Fang, X.; Mertens, R.; Pan, X.; Schuchmann, M. N.; Schuchmann, H.-P. *Water Sci. Technol.* **1997**, *35*, 9.
(36) Alfassi, Z. B.; Huie, R. E.; Neta, P. In *Peroxyl Radicals*; Alfassi, Z. B., Ed.; Wiley: Chichester, U.K., 1997; pp 235−281.
(37) Schuchmann, M. N.; von Sonntag, C. *J. Phys. Chem.* **1982**, *86*, 1995.
(38) Schuchmann, M. N.; von Sonntag, C. *J. Phys. Chem.* **1979**, *83*, 780.
(39) Russell, G. A. *J. Am. Chem. Soc.* **1957**, *79*, 3871.
(40) Atkinson, R. *Int. J. Chem. Kinet.* **1987**, *19*, 799.
(41) Small, R. D.; Scaiano, J. C. *J. Am. Chem. Soc.* **1978**, *100*, 296.
(42) Schuchmann, H.-P.; von Sonntag, C. *Z. Naturforsch.* **1984**, *39B*, 217.
(43) Bennett, J. E.; Summers, R. *Can. J. Chem.* **1974**, *52*, 1377.
(44) Onstein, P.; Stefan, M. I.; Bolton, J. R. *J. Adv. Oxid. Technol.* **1999**, *4*(2), 231.
(45) Asmus, K.-D.; Möckel, H.; Henglein, A. *J. Phys. Chem.* **1973**, *77*, 1218.

Received for review May 24, 1999. Revised manuscript received September 10, 1999. Accepted October 21, 1999.

ES9905748